Measurement of viscosity of lyotropic liquid crystals by means of rotating laser-trapped microparticles

Qingkun Liu,[1,2] Theodor Asavei,[3,4] Taewoo Lee,[1] Halina Rubinsztein-Dunlop,[3] Sailing He,[2,5] and Ivan I. Smalyukh[1,6,*]

[1]*Department of Physics, Material Science and Engineering Program, Department of Electrical, Computer, & Energy Engineering and Liquid Crystal Materials Research Center, University of Colorado, Boulder, CO 80309, USA*
[2]*Centre for Optical and Electromagnetic Research, Zhejiang University, Hangzhou 310058, China*
[3]*Quantum Science Laboratory, School of Physical Sciences, the University of Queensland, Brisbane QLD 4072, Australia*
[4]*School of Physics, Monash University, Clayton, Victoria 3800, Australia*
[5]*Department of Electromagnetic Engineering, Royal Institute of Technology, S-100 44 Stockholm, Sweden*
[6]*Renewable and Sustainable Energy Institute, National Renewable Energy Laboratory and University of Colorado, Boulder, CO 80309, USA*
[*]*ivan.smalyukh@colorado.edu*

Abstract: We describe a simple microrheology method to measure the viscosity coefficients of lyotropic liquid crystals. This approach is based on the use of a rotating laser-trapped optically anisotropic microsphere. In aligned liquid crystals that have negligible effect on trapping beam's polarization, the optical torque is transferred from circularly polarized laser trapping beam to the optically anisotropic microparticle and creates the shear flow in the liquid crystalline fluid. The balance of optical and viscous torques yields the local effective viscosity coefficients of the studied lyotropic systems in cholesteric and lamellar phases. This simple yet powerful method is capable of probing viscosity of complex anisotropic fluids for small amounts of sample and even in the presence of defects that obstruct the use of conventional rheology techniques.

OCIS codes: (140.7010) Laser trapping; (160.1190) Anisotropic optical materials; (160.3710) Liquid crystals; (180.1790) Confocal microscopy; (180.4315) Nonlinear microscopy; (180.6900) Three-dimensional microscopy; (350.4855) Optical tweezers or optical manipulation.

References and links

1. P. M. Chaikin and T. C. Lubensky, *Principles of Condensed Matter Physics* (Cambridge University Press, 2000).
2. K. F. Wissbrun, "Rheology of rod-like polymers in the liquid crystalline state," J. Rheol. (N.Y.N.Y.) **25**(6), 619–662 (1981).
3. I.-H. Lin, D. S. Miller, P. J. Bertics, C. J. Murphy, J. J. de Pablo, and N. L. Abbott, "Endotoxin-induced structural transformations in liquid crystalline droplets," Science **332**(6035), 1297–1300 (2011).
4. S. J. Woltman, G. D. Jay, and G. P. Crawford, "Liquid-crystal materials find a new order in biomedical applications," Nat. Mater. **6**(12), 929–938 (2007).
5. S. Sircar and Q. Wang, "Dynamics and rheology of biaxial liquid crystal polymers in shear flows," J. Rheol. (N.Y.N.Y.) **53**(4), 819–858 (2009).
6. D. Demus, J. Goodby, G. W. Gray, H.-W. Spiess, and V. Vill, eds., *Handbook of Liquid Crystals* (Wiley-VCH, 1998), Vol. 2A.
7. T. Thiele, J.-F. Berret, S. Müller, and C. Schmidt, "Rheology and nuclear magnetic resonance measurements under shear of sodium dodecyl sulfate/decanol/water," J. Rheol. (N.Y.N.Y.) **45**(1), 29–48 (2001).
8. J. Sato and V. Breedveld, "Transient rheology of solvent-responsive complex fluids by integrating microrheology and microfluidics," J. Rheol. (N.Y.N.Y.) **50**(1), 1–19 (2006).
9. A. I. Bishop, T. A. Nieminen, N. R. Heckenberg, and H. Rubinsztein-Dunlop, "Optical microrheology using rotating laser-trapped particles," Phys. Rev. Lett. **92**(19), 198104 (2004).
10. F. C. MacKintosh and C. F. Schmidt, "Microrheology," Curr. Opin. Colloid Interface Sci. **4**(4), 300–307 (1999).
11. G. Liao, I. I. Smalyukh, J. R. Kelly, O. D. Lavrentovich, and A. Jákli, "Electrorotation of colloidal particles in liquid crystals," Phys. Rev. E Stat. Nonlin. Soft Matter Phys. **72**(3), 031704 (2005).

#155473 - $15.00 USD Received 27 Sep 2011; accepted 11 Nov 2011; published 23 Nov 2011

12. J. C. Loudet, P. Hanusse, and P. Poulin, "Stokes drag on a sphere in a nematic liquid crystal," Science **306**(5701), 1525 (2004).
13. H. F. Gleeson, T. A. Wood, and M. Dickinson, "Laser manipulation in liquid crystals: an approach to microfluidics and micromachines," Philos. Trans. R. Soc. A Math. Phys. Eng. Sci. **364**(1847), 2789–2805 (2006).
14. M. E. J. Friese, T. A. Nieminen, N. R. Heckenberg, and H. Rubinsztein-Dunlop, "Optical alignment and spinning of laser-trapped microscopic particles," Nature **394**(6691), 348–350 (1998).
15. S. J. Parkin, R. Vogel, M. Persson, M. Funk, V. L. Loke, T. A. Nieminen, N. R. Heckenberg, and H. Rubinsztein-Dunlop, "Highly birefringent vaterite microspheres: production, characterization and applications for optical micromanipulation," Opt. Express **17**(24), 21944–21955 (2009).
16. L. J. Yu and A. Saupe, "Liquid crystalline phases of the sodium decylsulfate/decanol/water system. Nematic-nematic and cholesteric-cholesteric phase transitions," J. Am. Chem. Soc. **102**(15), 4879–4883 (1980).
17. A. M. Figueiredo Neto and S. R. A. Salinas, *The Physics of Lyotropic Liquid Crystals* (Oxford University Press, 2005).
18. Q. Liu, C. Beier, J. Evans, T. Lee, S. He, and I. I. Smalyukh, "Self-alignment of dye molecules in micelles and lamellae for three-dimensional imaging of lyotropic liquid crystals," Langmuir **27**(12), 7446–7452 (2011).
19. I. I. Smalyukh, S. Shiyanovskii, and O. D. Lavrentovich, "Three-dimensional imaging of orientational order by fluorescence confocal polarizing microscopy," Chem. Phys. Lett. **336**(1-2), 88–96 (2001).
20. R. Bartolino, T. Chiaranza, M. Meuti, and R. Compagnoni, "Uniaxial and biaxial lyotropic nematic liquid crystals," Phys. Rev. A **26**(2), 1116–1119 (1982).
21. S. Dominguez Bella and J. M. Garcia-Ruiz, "Textures in induced morphology crystal aggregates of CaCO3: sheaf of wheat morphologies," J. Cryst. Growth **79**(1-3), 236–240 (1986).
22. R. Vogel, M. Persson, C. Feng, S. J. Parkin, T. A. Nieminen, B. Wood, N. R. Heckenberg, and H. Rubinsztein-Dunlop, "Synthesis and surface modification of birefringent vaterite microspheres," Langmuir **25**(19), 11672–11679 (2009).
23. V. L. Y. Loke, T. A. Nieminen, S. J. Parkin, N. R. Heckenberg, and H. Rubinsztein-Dunlop, "FDFD/T-matrix hybrid method," J. Quant. Spectrosc. Radiat. Transf. **106**(1-3), 274–284 (2007).
24. T. A. Nieminen, N. R. Heckenberg, and H. Rubinsztein-Dunlop, "Optical measurement of microscopic torques," J. Mod. Opt. **48**, 405–413 (2001).
25. T. Lee, R. P. Trivedi, and I. I. Smalyukh, "Multimodal nonlinear optical polarizing microscopy of long-range molecular order in liquid crystals," Opt. Lett. **35**(20), 3447–3449 (2010).
26. R. P. Trivedi, T. Lee, K. A. Bertness, and I. I. Smalyukh, "Three dimensional optical manipulation and structural imaging of soft materials by use of laser tweezers and multimodal nonlinear microscopy," Opt. Express **18**(26), 27658–27669 (2010).
27. M. Kuzman, Y. W. Hui, and M. M. Labes, "Capillary viscometry of some lyotropic nematics," Mol. Cryst. Liq. Cryst. (Phila. Pa.) **172**, 211–215 (1989).

1. Introduction

Liquid crystals (LCs) are a class of technologically important anisotropic complex fluids with long-range orientational and partial or no positional ordering of molecules or other building blocks such as micelles, nanoparticles, and molecular stacks. Their mean local orientation is described by the so-called director **n** with non-polar symmetry and **n** being indistinguishable from **–n** [1]. The rheology of anisotropic fluids has attracted both theoretical and applied interest because of its significance for many applications such as displays [1–4], biodetectors [3,4], processing of LC polymers [2,5], etc. For example, lower viscosity coefficients allow for faster switching of displays and electro-optic devices [4–6]. Since the mechanical response of LCs depends on the orientation of **n** with respect to the shear, velocity, and velocity gradient directions, hydrodynamics of defect-free LCs is complicated and its theoretical description usually relies on the use of three Miesowicz shear viscosity coefficients. It also relies on six Leslie flow viscosity coefficients (five of which are independent), and a rotational viscosity coefficient that do not have analogues in the regular isotropic fluids [1]. However, the rheological properties of LCs are also dependent on the details of spatially non-uniform director structures and defects in the long-range self-assembly of the LC building blocks and a reliable experimental measurement of some "effective" flow viscosity coefficient is notoriously difficult [6–8].

Various methods have been employed to measure the viscosity coefficients of LCs, such as capillary flow [6], dynamic light scattering [6], nuclear magnetic resonance (NMR) [7], particle tracking microrheology, and microfluidics [8]. However, their application is often limited by the presence of defects and the difficulty of proper control of LC alignment during the rheological studies. Therefore, probing the complicated interplay of flow and mesoscopic structure in LCs during flow and its influence on the fluid's rheology is a technical challenge.

#155473 - $15.00 USD Received 27 Sep 2011; accepted 11 Nov 2011; published 23 Nov 2011

It is impossible to use the conventional methods based on the bulk LCs with uniform orientation to perform the rheological study on micro- and nano-scales and for small amounts of the material.

Laser tweezers and optically trapped rotating microspheres have been previously used to probe complex fluids (including thermotropic LCs) at mesoscales [9–13]. For example, the rotating-particle microrheological method based on laser tweezers has been used for measuring the viscosity of fluids such as water and cellular sap [9]. In this work, we extend this rotating-particle method of Friese *et al.* [14] and Bishop *et al.* [9] to the study of LC fluids and measure effective viscosity coefficients of these complex soft matter systems. Instead of applying the laminar flow of LCs, we rotate an optically anisotropic microsphere by means of a trapping laser beam to exert shear stress on the surroundings. Circularly polarized light carrying the spin angular momentum (SAM) allows us to apply a torque and rotate a microparticle by means of an exchange of optical angular momentum (OAM) between the beam and the object [14,15]. We utilize a rotating laser-trapped optically anisotropic microsphere to locally measure the effective viscosity of lyotropic LC fluids in cholesteric and lamellar phases. This method does not require perfectly aligned samples (which are difficult to achieve for lyotropic LCs), avoids artifacts such as those due to defects, and can be used when only tiny amounts of the sample are available.

2. Sample preparation

We study lyotropic LCs in cholesteric and lamellar phases of sodium decyl sulfate-decanol-water (SDS/1-decanol/water) ternary system with well-established phase diagram [16,17]. The LC in cholesteric phase was prepared using a composition of 35.5 wt% of SDS, 7.5 wt% of 1-decanol (both used as supplied from Aldrich), 56 wt% of deionized water and 1 wt% of chiral agent brucine sulfate heptahydrate (BSH). The mixing of these constituents was followed by ultrasonication for 2 hours at room temperature. The pitch p [distance along the helical axis over which micelles twist by 2π, Fig. 1(a)] of the used cholesteric LC was chosen to be about 10μm. The cell confinement typically yields planar-aligned cholesteric structures with some oily streaks defects, Figs. 1(a) and (c). The LC in the lamellar phase was prepared as described above for the cholesteric case but consisted of 28 wt% of SDS, 8 wt% of 1-decanol, and 64 wt% of water. The ternary lyotropic system with this composition self-organized as a two dimensional lamellar fluid with the lamellae aligned predominantly parallel to the confining glass plates (except for the regions with defects such as dislocations, oily streaks, and focal conic domains), Figs. 1(b) and (d). About 0.01 wt% of the fluorescent dye $DiOC_{18}(3)$ (3, 3′-dioctadecyloxacarbocyanine perchlorate, obtained from Invitrogen) was added to some of the studied samples for the polarized fluorescence-based imaging of director structures in the cholesteric and lamellar LCs [18,19]. The average refractive index of the used ternary system is within 1.37-1.39, depending on the exact composition and the mesophase [20]. In general, the values of the effective LC refractive index depend on the polarization and the propagating direction of light with respect to $\mathbf{n}(\mathbf{r})$, varying between the so-called "ordinary" n_o and "extraordinary" n_e refractive indices. However, optical anisotropy of these lyotropic LCs is very small: $|\Delta n_{LC}| = |n_e - n_o| < 0.006$.

The highly birefringent spherical microparticles were obtained by means of self-assembly of calcium carbonate using a protocol described in details elsewhere [21,22]. This procedure yields the so-called "vaterite" microparticle that can withstand considerable torques and laser powers when rotated by circularly polarized laser light. Their absorption at the trapping laser wavelength is very low. The diameters of the obtained birefringent beads are usually between 3μm and 10μm, Fig. 2(c). These birefringent beads were suspended in the LCs which were sandwiched between two confining glass plates about 100μm apart and sealed together with epoxy glue. The internal structure of an axially-symmetric vaterite microparticle with the symmetry axis aligned along the x-direction is shown in Fig. 2(d) [23]. The birefringence of the colloidal vaterite, Fig. 2(a, b) allows for the transfer of SAM from a circularly polarized laser beam to the microparticle, which causes its rotation at a constant angular velocity

#155473 - $15.00 USD Received 27 Sep 2011; accepted 11 Nov 2011; published 23 Nov 2011

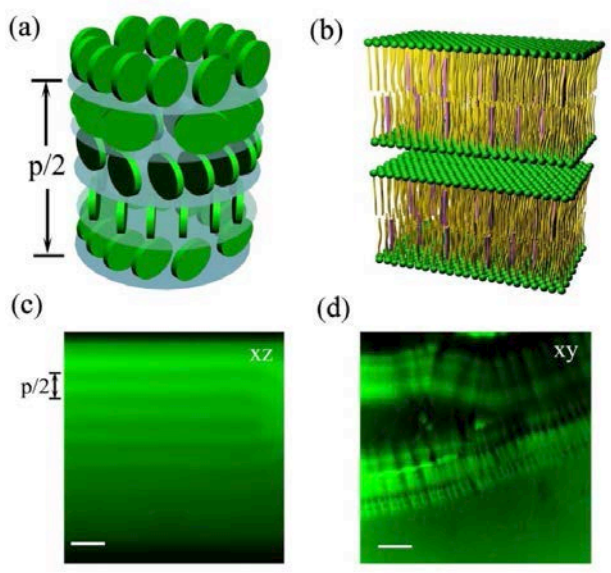

Fig. 1. Schemes of (a) cholesteric LC phase formed by self-aligned disc-shaped micelles and (b) lamellar LC phase formed by bilayers. FCPM images of (c) cholesteric LC in the vertical cross-section and (d) lamellar LC in the in-plane cross-section. The scale bars in (c, d) are 10μm.

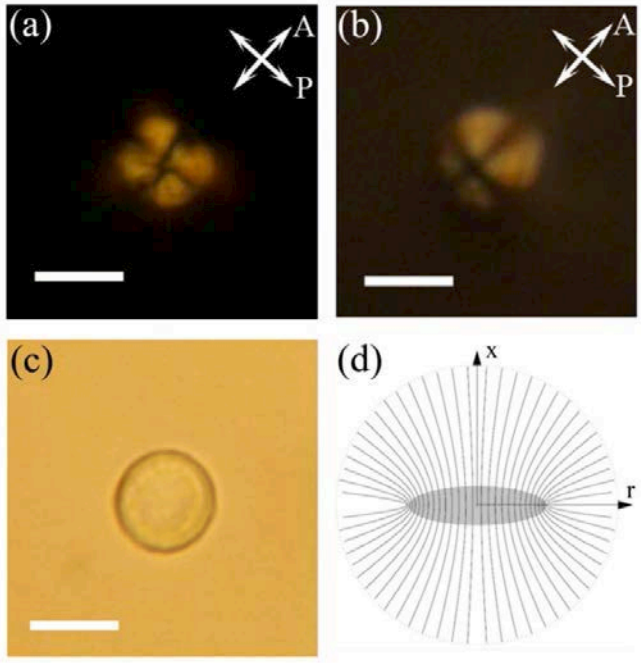

Fig. 2. Polarized optical microscopy images of beads in (a) cholesteric and (b) lamallar LC phases. P: polarizer, A: analyzer (c) A bright-field transmission image of the bead in water. (d) The structure of the spatial pattern of the optical axis within the bead; note that the particle has rotational symmetry and is invariant with respect to rotation around **x**-axis marked on the schematic. The scale bar in (a-c) is 10μm. The diameters of the beads used in the experiments are varied between 3μm and 10μm.

#155473 - $15.00 USD Received 27 Sep 2011; accepted 11 Nov 2011; published 23 Nov 2011

determined by the balance of viscous and optical torques and thus allows one to measure the viscous drag force and an effective viscosity coefficients for purely viscous fluid. The effective birefringence of the vaterite particles Δn_v is about 0.06 [15], which is about an order of magnitude larger than that of used lyotropic LCs.

3. Optical tweezers and imaging techniques

Optical trapping is performed using an inverted microscope with a 100× oil immersion objective lens with high numerical aperture (NA = 1.3) integrated with a charge coupled device (CCD) camera, Fig. 3(a). The power of laser beam at 1070nm from an Ytterbium fiber laser (IPG Photonics) is controlled by a half-wave plate (λ/2) and a polarizer and then the light is focused to a diffraction-limited spot in the sample by the objective. A quarter-wave plate (λ/4) located immediately before the objective converts the linearly polarized light into a circularly polarized beam that is then used to rotate birefringent objects, Fig. 3(b). After passing through the particle, the laser light is collected by a condenser and then split into two orthogonal linearly polarized beams by another quarter-wave plate with the fast axis orientated at 45° to the axes of a polarizing beam-splitter (PBS) cube [9,24]. The two linearly polarized components correspond to the left-handed and right-handed circularly polarized light of the outgoing beam. The transmitted light is then measured by two photo detectors (PD1 and PD2) that are placed in the optical path after the PBS cube. The two photodiodes monitoring the intensities of the two orthogonal components of the beams after the PBS provide a measure of the degree of circular polarization in the outgoing light, which allows one to measure the change in angular momentum. These measurements yield information about the torque applied to the particle. The frequency of rotation of the particle is also accurately determined by monitoring the light intensity changes measured by photodiodes.

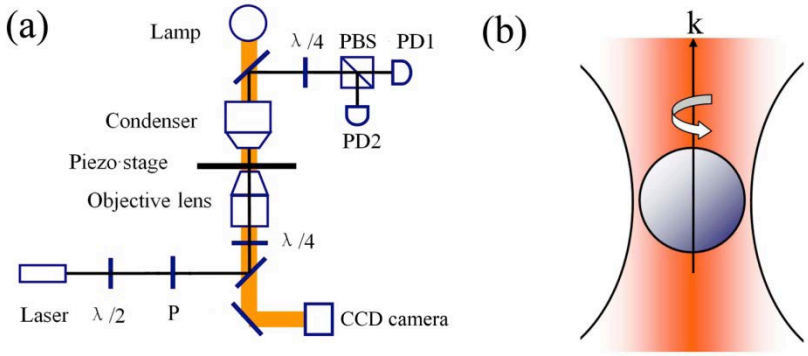

Fig. 3. (a) Experimental setup and (b) schematic of laser trapping by circularly polarized beam causing particle rotation. PBS: polarizing beam-splitter, PD: photo detector, P: polarizer, λ/2: half-wave plate, λ/4: quarter-wave plate, **k**: wave vector of incident light.

Optical polarizing microscopy textures of the LCs with and without immersed microparticles are investigated by inserting a set of two orthogonally aligned polarizers into the setup and removing the quarter-wave plate from the optical path. The textures of the planar-aligned cholesteric LC and homeotropically aligned lamellar LC are shown in Fig. 1(c, d), respectively. The fluorescence confocal polarizing microscopy (FCPM) setup is built on a laser scanning confocal microscope (Olympus FV 300 with IX-81) supplemented with a twisted-nematic achromatic linear polarization rotator. The excitation beam (488nm, Ar-ion laser) is focused by an objective into a small volume (<1 μm^3) in the sample. The fluorescence signal of dye molecules from this volume is detected by a photomultiplier tube in the spectral region of 510-550 nm selected by interference filters. The use of a pinhole in the detection channel (located in a plane confocal with the focal plane of the objective) of the fluorescence confocal microscope allows one to achieve submicron resolution along the optical axis of the microscope, in addition to the similar diffraction-limited resolution in the

#155473 - $15.00 USD Received 27 Sep 2011; accepted 11 Nov 2011; published 23 Nov 2011

lateral plane of the microscope. The three-dimensional (3D) **n**(**r**) around colloids is also determined with submicron lateral and vertical resolution by use of an anisotropic fluorescent dye and detecting the polarized fluorescence signal using FCPM. We have also utilized two-photon excitation fluorescence polarizing microscopy (2PEF-PM) for imaging of **n**(**r**) patterns and spatial location of the microparticles used as microrheology probes. This technique constitutes of the multimodal nonlinear polarizing microscopy described in details elsewhere [25,26]. The 2PEF-PM imaging is performed by use of excitation with a 960nm femtosecond pulse from a tunable (680-1080 nm) Ti:sapphire oscillator (140 fs, 80 MHz, Chameleon Ultra-II, Coherent). We use epi-detection mode and interference filters to separate the fluorescent signal from the excitation light [19]. This nonlinear optical process of two-photon absorption of the dye molecules attains the high intrinsic submicron resolution in both axial and radial direction as well as a stronger sensitivity to molecular orientations as compared to FCPM [25,26]. FCPM and 2PEF-PM imaging was performed by using a 100 × objective with NA = 1.4 or a 60× objective with NA = 1.42 and yield consistent results; the simultaneous imaging with these techniques allows us to avoid or mitigate the effect of different artifacts (such as the Mauguin effect following of light polarization) that can be encountered when using these techniques [6,18].

4. Results and discussion

The effective LC viscosity coefficient is estimated by probing the balance of the optical torque exerted on the particle by a focused laser beam and the viscous drag torque dependent on the fluid viscosity. Since the Reynolds number is low ($Re \sim 10^{-7}$), the inertia effects are negligible [1]. Furthermore, since the Erickson number is also much smaller than unity, the perturbations of **n**(**r**) due to the fluid flow caused by the microsphere rotation can be ignored [1]. We therefore measure the optical torque and the rotation frequency as first considered by Nieminen *et al*. [24] and described in details by Bishop *et al*. [9]. The optical torque applied to the particle is determined by measuring the difference between the initial degree of circular polarization of the beam in the absence of the particle and the final polarization state:

$$\tau_{optical} = \Delta\sigma P / \omega$$

where $\Delta\sigma$ is the change in the degree of circular polarization as the beam passes through the particle, P is the laser power, and ω is the optical angular frequency. We have verified that the change of the degree of polarization of light passing through the lyotropic cholesteric LC (with the helical axis along the cell normal) is less than 2% and this change is less than 0.1% in the case of the lamellar LC with layers parallel to the LC cell's glass substrates (i.e., the effect of the aligned LC in this geometry on polarization can be neglected) The effective viscosity coefficient η is found by equating the optical torque and the viscous drag torque applied on the rotating sphere:

$$\eta = \Delta\sigma P / (8\pi a^3 \Omega\omega)$$

where a is the radius of the sphere and Ω is the angular frequency of its rotation.

The use of microrheology methods for the viscosity measurement in LC fluids is generally much more complicated than in the case of isotropic media and a number of precautions are needed to preclude possible artifacts [11–13]. The main sources of possible problems arising in the case of our rotating-particle method are: (i) defects forming around a particle (or simply happening to be in the proximity of it) can modify the LC's mechanical response; (ii) significant changes of light polarization state due to the fact that the trapping beam is traversing the anisotropic LC medium before and after the propagating through the trapped particle. However, these artifacts can be avoided or mitigated by a careful design of the experiment. Polarizing microscopy textures shown in Figs. 2(a), (b) and 2PEF-PM textures in Fig. 4 similar to the ones shown in Figs. 1(c), (d) indicate that the used colloids do not significantly perturb **n**(**r**) of the uniform lamellar and planar cholesteric textures in the respective phases. With the laser tweezers, one can bring the probing microparticle to a

#155473 - $15.00 USD Received 27 Sep 2011; accepted 11 Nov 2011; published 23 Nov 2011

desired location within the 3D volume of the sample and in this way assure that the measurement is done in a region with a desired uniform **n**(**r**) and far away from defects, Fig. 4. On the other hand, the influence of defects on mechanical response of the LC can be probed by deliberately doing the microparticle rotation experiment in the proximity of defects which are rather abundant in lyotropic LCs (Fig. 4). The possible artifacts due to the optically anisotropic nature of LCs can be mitigated by aligning them to have a specific well-defined orientation of **n**(**r**) with respect to the optical axis of the microscope, like in the case of homeotropic alignment of the studied LC in the lamellar phase that has **n**(**r**) parallel to the axis of trapping laser beam [Fig. 1(b) and Fig. 2(b)] or planar alignment of cholesteric lamellae with the helical axis along the cell normal [Figs. 1(a), (c), Fig. 2(a), and Fig. 4(c), (f)].

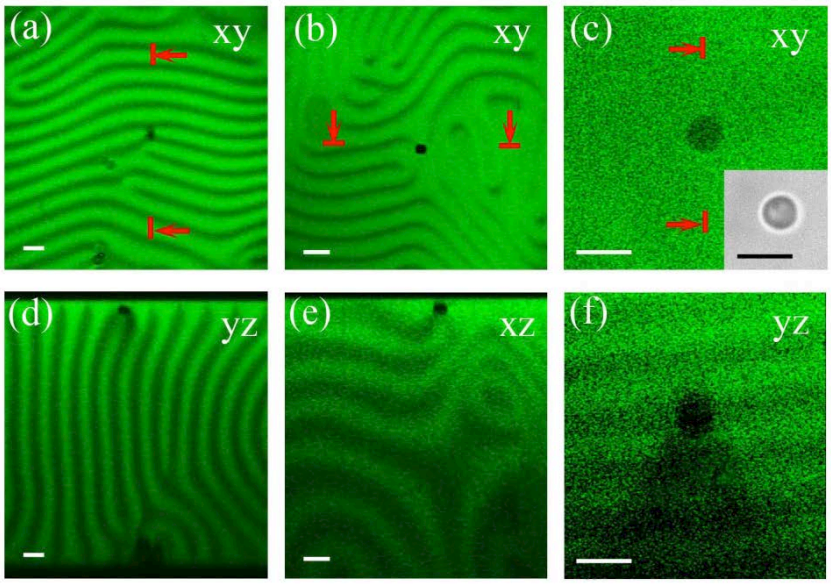

Fig. 4. 2PEF-PM images of vaterite in (a) homeotropically aligned cholesteric LC and (b) cholesteric LC under flow induced by pressing on the confining glass plates of LC cell. (c) 2PEF-PM images of a vaterite particle which has been moved by laser trapping to the center of the sample of planar-aligned cholesteric LC. The inset of (c) is the bright field image of the vaterite microparticle. The red lines in (a)-(c) indicate locations where the vertical cross sections (d)-(f) are taken respectively. The scale bars in all images are 5μm. Note that the microparticles in (a, b, d, e) spontaneously localize into the LC defect regions to minimize the overall elastic free energy due to defects and elastic distortions induced by the beads.

In the planar-aligned cholesteric LC, the helical axis coincides with the axis of rotation of the bead. In this configuration, the helical axis is also normal to shear velocity and the shear gradient, so that the rotating bead does not significantly modify the director structure. In the experiment, the bead is first spatially manipulated and localized in the center of the LC cell [Figs. 4(c), (f)] by the trapping laser beam and then rotated once the polarization is switched from linear to circular. Due to the very low birefringence of the LCs $\Delta n_{LC} < 0.01$, the so-called Mauguin parameter $M_{au} = p\Delta n_{LC}/(2\lambda)$ is much smaller than unity and the light propagation in the cholesteric LC is far from the Mauguin regime (here λ is the wavelength of trapping light) [6,18]. Furthermore, the LC medium's effect on circular trapping beam's polarization can be neglected. The photodiodes PD1 and PD2 are calibrated such that they provide a measure of the power at the trapping focus under the assumption that all of the transmitted light is collected by the condenser. The output voltages measured by the detectors PD1 and PD2 yield relative optical power of the two circularly polarized components. In agreement with the above hypothesis about the LC medium's effect on light polarization, after the left-handed circularly polarized incident laser light propagates through the cholesteric LC

#155473 - $15.00 USD Received 27 Sep 2011; accepted 11 Nov 2011; published 23 Nov 2011

sample in the absence of the birefringent bead, its polarization state remains unperturbed, indicating that the possible optical artifacts due to the LC medium can be neglected. When this light propagates through the trapped bead, the optical axis of the bead aligns parallel to the beam's lateral plane due to the anisotropic optical forces. As the particles starts rotating when trapped by a circularly polarized beam, the measured output light is modulated by the rotating bead that alters polarization of the beam similar to the case of a rotating wave plate. The substantial depth of modulation is enabled by the large diameter of the chosen bead, larger than the waist of the trapping beam. The change of the degree of circular polarization and the rotation frequency are extracted from the intensity vs. time data measured by PD1 and PD2. The frequency of the intensity signals measured by PD1 and PD2 is twice the rotation speed of the beads. Using experimental data shown in Fig. 5(a), we find that the viscosity of the cholesteric LC is 39.8 cP. This viscosity is of the same order of magnitude (although approximately half of the value) as that measured by capillary method and previously reported in literature for a similar ternary system but without a chiral additive (i.e., in a nematic rather than cholesteric phase) [27]. The difference can be explained by the facts that the composition of the used lyotropic LC is somewhat different and that our measurement is performed for a well-defined geometry with particle rotation around an axis perpendicular to **n**(**r**) and parallel to the cholesteric's helical axis. The other reason is that the local viscosity measured by our method precludes the influence of defects that may increase the viscosity of the bulk LC sample in capillary viscometry. Since the defects and poorly controlled alignment are expected to increase viscosity values and since the dependence of viscosity coefficients in LCs on the mutual alignment of the **n**(**r**), velocity, and velocity gradient is typically substantial, our measured effective viscosity is generally consistent with the previous studies [27].

By changing the laser power, we probe the values of effective LC viscosity as we vary the shear stress, Fig. 5(b). It can be seen from this figure that we do not observe any significant change of viscosity with increasing laser power, indicating the presence of a laminar flow around the bead and no significant heating effect present up to laser power of 0.89 W and the shear speeds up to 4.4 μm/s. This shows the stability of this method in a wide range of laser power values. Furthermore, this is also consistent with the fact that there is no significant heating or laser-induced realignment of the LC director at such high laser powers.

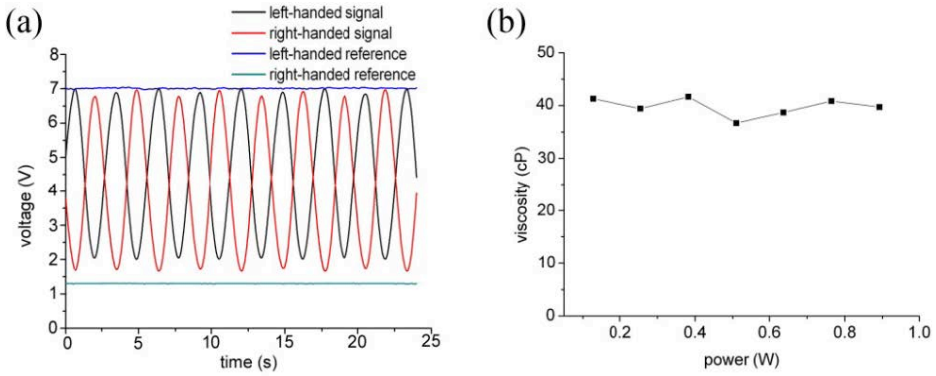

Fig. 5. (a) Intensity signal of circularly polarized light after passing through the vaterite particle in a lyotropic LC in cholesteric phase while the bead is being trapped by a beam of power 0.89W. (b) The viscosity coefficient measured at different powers of the trapping laser beam; the viscosity variations with power are comparable to the measurement error of about 6 cP.

The lamellar LCs can be considered both as a two-dimensional liquid and a one-dimensional solid since the orientational order in these soft matter systems is supplemented by the quasi-long-range one-dimensional positional ordering. This layered system, therefore, exhibits very different mechanical response depending on the direction of the applied stress with respect to **n**(**r**) and the layers. Since the system's response is fluid-like within the layers

#155473 - $15.00 USD Received 27 Sep 2011; accepted 11 Nov 2011; published 23 Nov 2011

and the bead is rotating around an axis normal to the lamellae, the geometry of our experiment assures that the velocity and velocity gradient directions are parallel to the layers (since the shear flow created by the rotating vaterite is parallel to the layers). We have also assured that the lamellar LC with homeotropic **n**(**r**) along the trapping beam's axis has no measurable effect on circular polarization of the used trapping light. The vaterite particle causes weaker modulation of the circularly polarized laser light intensity in lamellar phase (Fig. 6) than what was observed in the previous experiment (Fig. 5), because of its smaller diameter (4.5 μm) of the used particle as compared to the case of viscosity measurements in a cholesteric LC where the vateriate was approximately 10 μm. The measured effective viscosity coefficient of the lyotropic LC in the lamellar phase is 23.4 cP. In obtaining this value, we have assured that there are no LC defects in the proximity of the particle which defects are rather common in lamellar LCs and can be seen in the image shown in Fig. 1(d) and that no defects are formed due to the incorporation of this particle into the lyotropic LC [Fig. 1(b)], although such defects are observed being induced by colloidal inclusions in the thermotropic smectics [11]. Therefore, the inaccuracy of these viscosity measurements in LCs, similar to the case of isotropic fluids, is determined predominantly by the measurement of the radius a of the vaterite bead (measured using optical microscopy images like the one shown in Fig. 2c), since viscosity scales as $\eta \propto a^{-3}$.

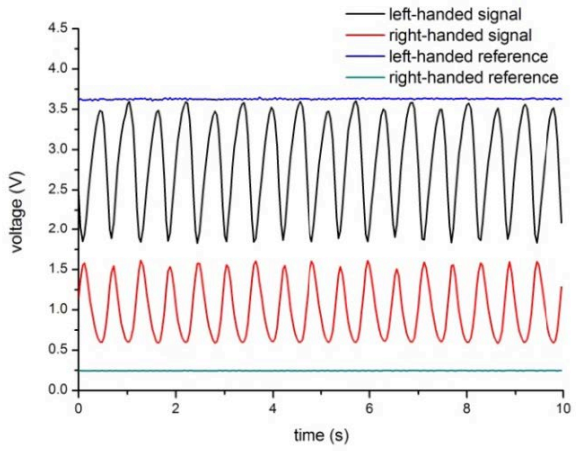

Fig. 6. Intensity signals of circularly polarized light after passing through the vaterite particle in a lyotropic LC in lamellar phase.

5. Conclusion

To conclude, we have measured the effective viscosity coefficients of lyotropic LCs in cholesteric and lamellar phases using a rotating optically trapped birefringent microparticle and the laser tweezers method. Since the electrically-induced so-called "Quincke rotation" can be only obtained in certain fluids and not in water-based LCs, our technique is of especially great interest for the study of a broad range of lyotropic LCs, such as those based on DNA, chromonic aggregates, surfactant micelles, etc. The use of this method can be also further extended to microrheology studies of other LC fluids, such as thermotropic LCs, polymer melts, provided that these LC fluids can be aligned in such a way that their influence on the trapping light's polarization state can be neglected (i.e., by means of using LCs aligned with the director along the axis of the trapping laser beam). When using this approach in the study of thermotropic LCs, which typically exhibit a facile response to focused high-power laser beams, one will need to assure that the used laser powers are low enough so that there is no laser-induced realignment of the LC director. We expect that our approach will greatly

#155473 - $15.00 USD Received 27 Sep 2011; accepted 11 Nov 2011; published 23 Nov 2011

impinge on the rheological studies of LCs made of nanoparticles and newly-synthesized organic molecules, which are often available only in tiny μl-level amounts. Our method also allows one to avoid the effects of presence or flow-induced generation of defects on viscosity measurements. At the same time, it can be also used to probe how defects modify mechanical response of various LC fluids. From the standpoint of view of the rheological study of lyotropic LCs, the main advantage of our method as compared to the passive particle microrheology techniques is that the spatial position of particles within the sample as well as velocity and velocity gradient directions with respect to the LC director can be controlled, so that the influence of low-quality alignment (inherent to lyotropic LCs) or effects of particle localization into defects can be mitigated.

Acknowledgments

This work was supported by the International Institute for Complex Adaptive Matter (ICAM-I2CAM), Renewable and Sustainable Energy Initiative and Innovation Initiative Seed Grant Programs of University of Colorado, the NSF grants DMR 0645461, DMR-0820579 and DMR-0847782, the National Basic Research program of China (2004CB719800) and the Australian Research Council. We thank Paul Ackerman, Noel Clark, Angel Martinez, Julian Evans, and Rahul Trivedi for discussions. We also thank Bohdan Senyuk for his help with the 2PEF-PM imaging experiments.

#155473 - $15.00 USD Received 27 Sep 2011; accepted 11 Nov 2011; published 23 Nov 2011